

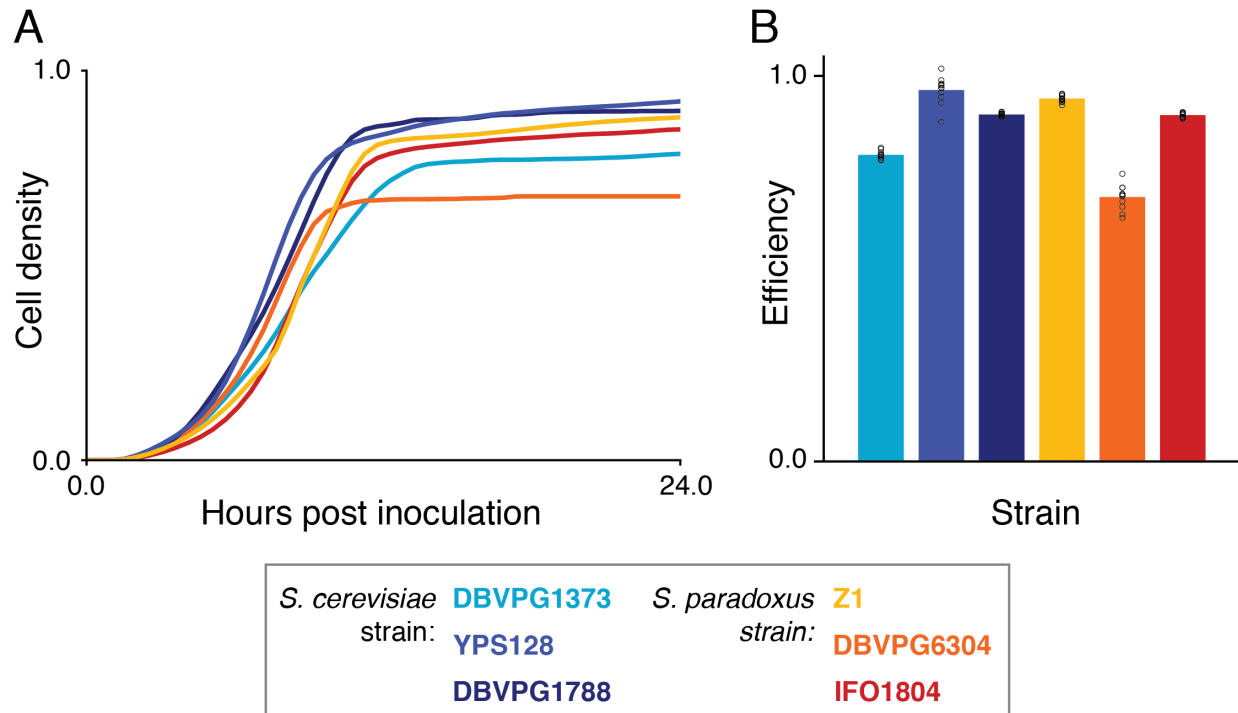
Extended data

Figures S1-S10

Tables S1-S4

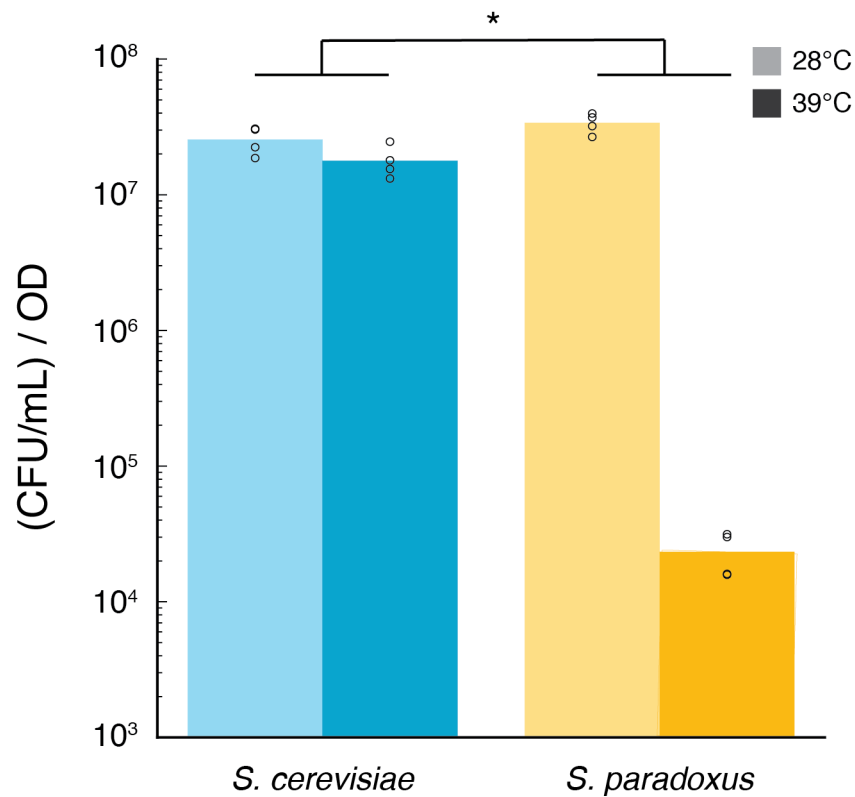
Supplementary figures

Supplementary Figure 1



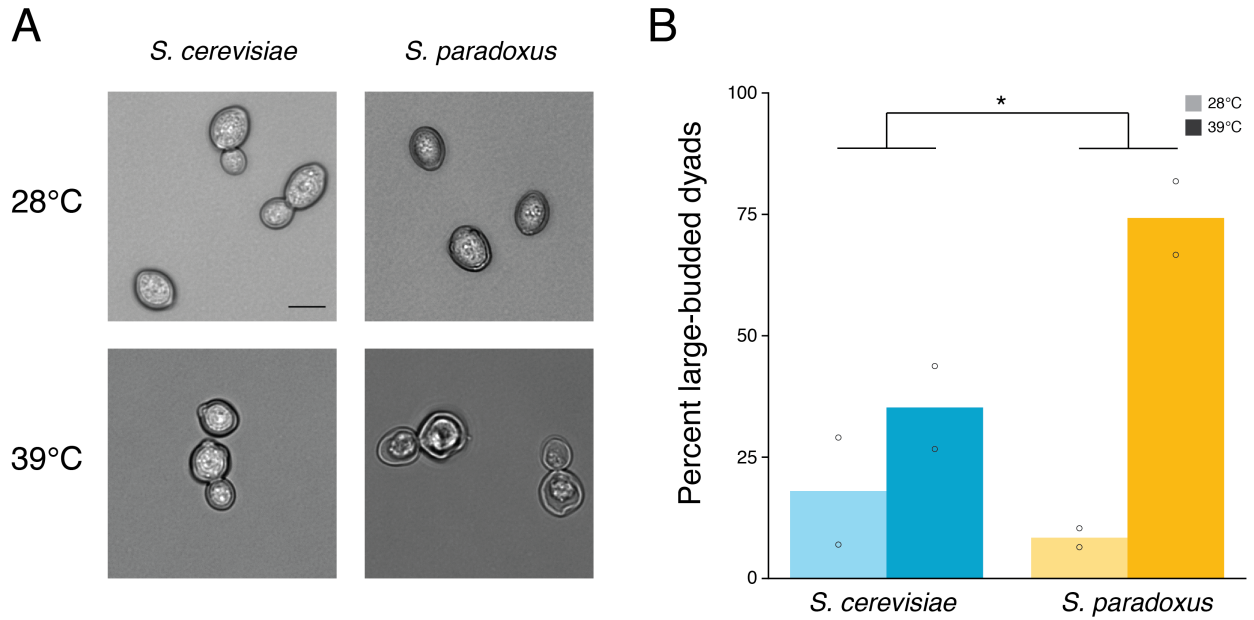
Supplementary Figure 1. *S. cerevisiae* and *S. paradoxus* do not differ significantly with respect to growth at 28°C. **A**, Each trace reports mean optical density (OD₅₉₅) over time of the indicated wild isolate of *S. cerevisiae* (blue) or *S. paradoxus* (orange) cultured at 28°C ($n \geq 11$). **B**, Each bar reports the mean efficiency ($n \geq 11$) of the indicated strain after 24 hours of growth at 28°C; individual measurements are reported as open circles. Efficiencies across strains were not significantly different between the species ($p = 0.07$).

Supplementary Figure 2



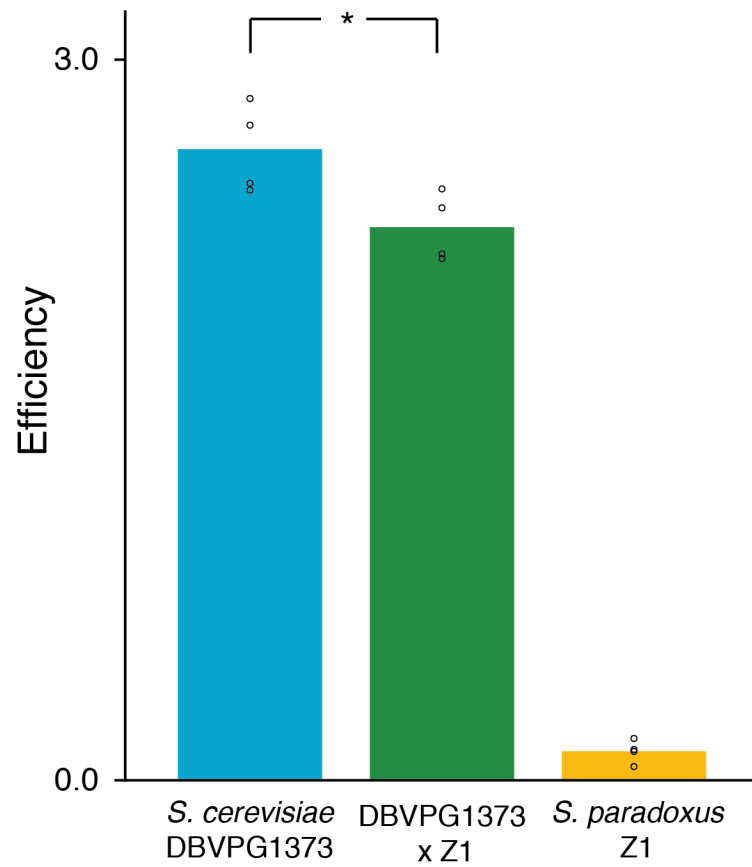
Supplementary Figure 2. Survival of *S. cerevisiae* cells is higher than that of *S. paradoxus* at 39°C. Each pair of bars reports the mean number of colony-forming units, per mL of culture per unit of cell density (OD_{600}), from a liquid culture of *S. cerevisiae* DBVPG1373 or *S. paradoxus* Z1 grown for 24 hours at the indicated temperature ($n = 4$). *, interaction $p = 0.00015$ in an ANOVA with species and temperature as factors; individual replicates are reported as open circles.

Supplementary Figure 3



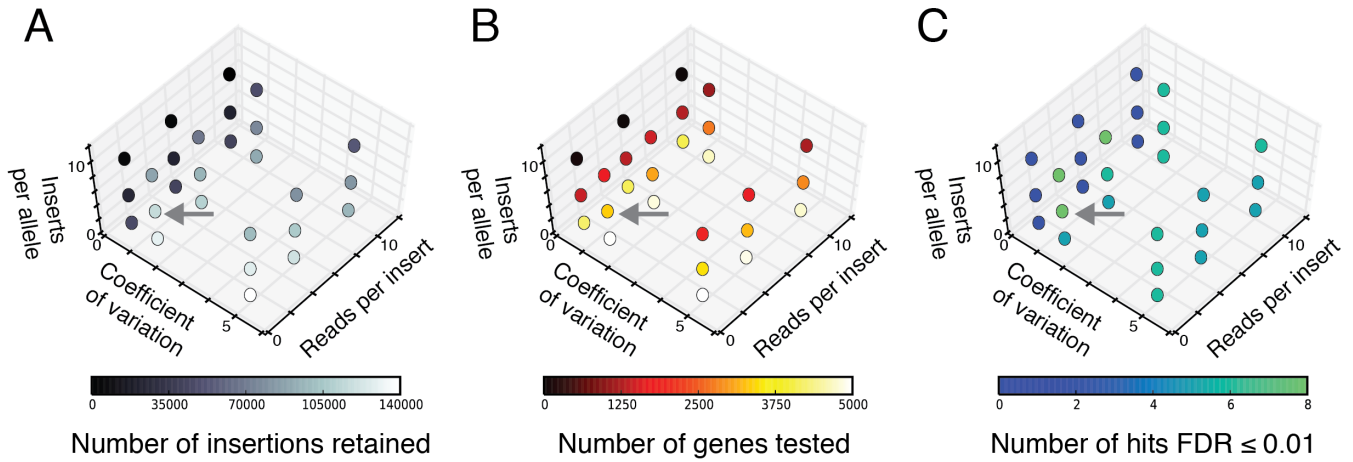
Supplementary Figure 3. *S. paradoxus* cells are predominantly large-budded dyads at high temperature. Each panel reports results from microscopy experiments of *S. cerevisiae* DBVPG1373 and *S. paradoxus* Z1 after 24 hours of liquid growth at the indicated temperature; at 28°C, both species were approaching stationary phase. **A**, Representative images. Scale bar, 5 μ m. **B**, Each pair of bars reports the proportion of large-budded dyads, as a mean across replicate cultures ($n = 2$), in the indicated species and temperature. *, interaction $p = 0.038$ in an ANOVA with species and temperature as factors; individual replicates are reported as open circles.

Supplementary Figure 4



Supplementary Figure 4. Growth of the *S. cerevisiae* x *S. paradoxus* hybrid is between that of its purebred parents at 39°C. Each bar reports the mean efficiency of the indicated strain ($n = 4$) after 24 hours of growth at 39°C; individual measurements are reported as open circles. *, $p = 0.035$.

Supplementary Figure 5



Supplementary Figure 5. Dependence of the RH-seq data set on cutoffs for read depth

and transposon mutant coverage. A, The x-axis reports the average number of sequencing

reads mapping to a given transposon insertion in either the 28°C or 39°C selection, as a

minimum level above which the insertion was retained for analysis. The y-axis reports the

coefficient of variation of read abundances between biological replicates for a given transposon

insertion, as a maximum level below which the insertion was retained for analysis. The z-axis

reports the number of transposon insertions per allele, as a minimum above which the gene was

retained for analysis. The color of each circle reports the number of insertions retained for

analysis in the indicated cutoff scheme. **B,** Data and symbols are as in **A**, except that the color

of each circle reports the number of genes retained for analysis in the indicated cutoff scheme.

C, Data and symbols are as in **A**, except that the color of each circle reports the number of

genes that scored below a p -value corresponding to a false-discovery rate (FDR) of 0.01 in the

reciprocal hemizyosity test using RH-seq data, in the indicated cutoff scheme. Arrows indicate

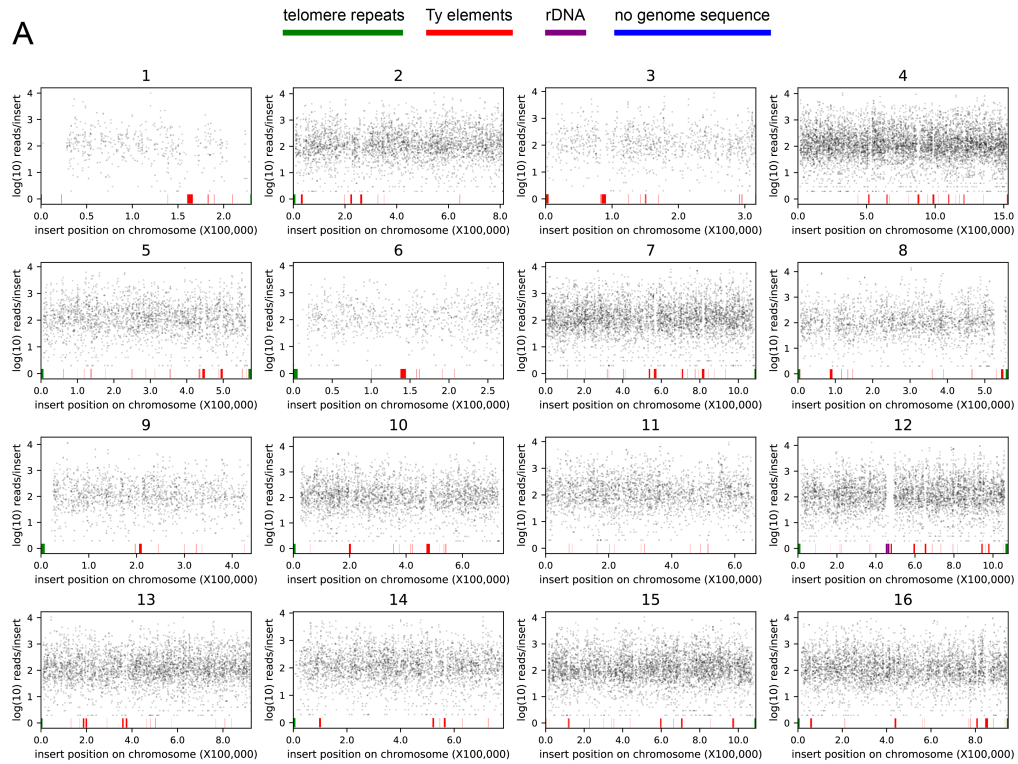
the set of cutoff values used in this study, which yielded a dataset of 110,678 usable insertions

across 3416 analyzable genes, 8 of which scored below FDR = 0.01 in the reciprocal

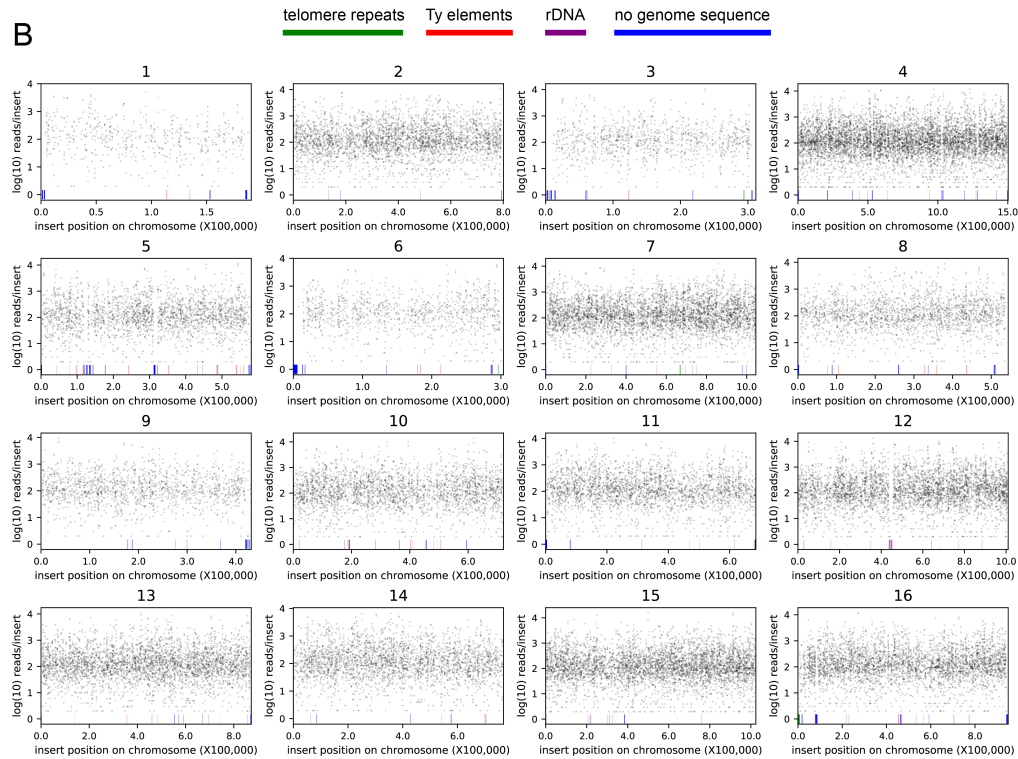
hemizyosity test.

Supplementary Figure 6

A

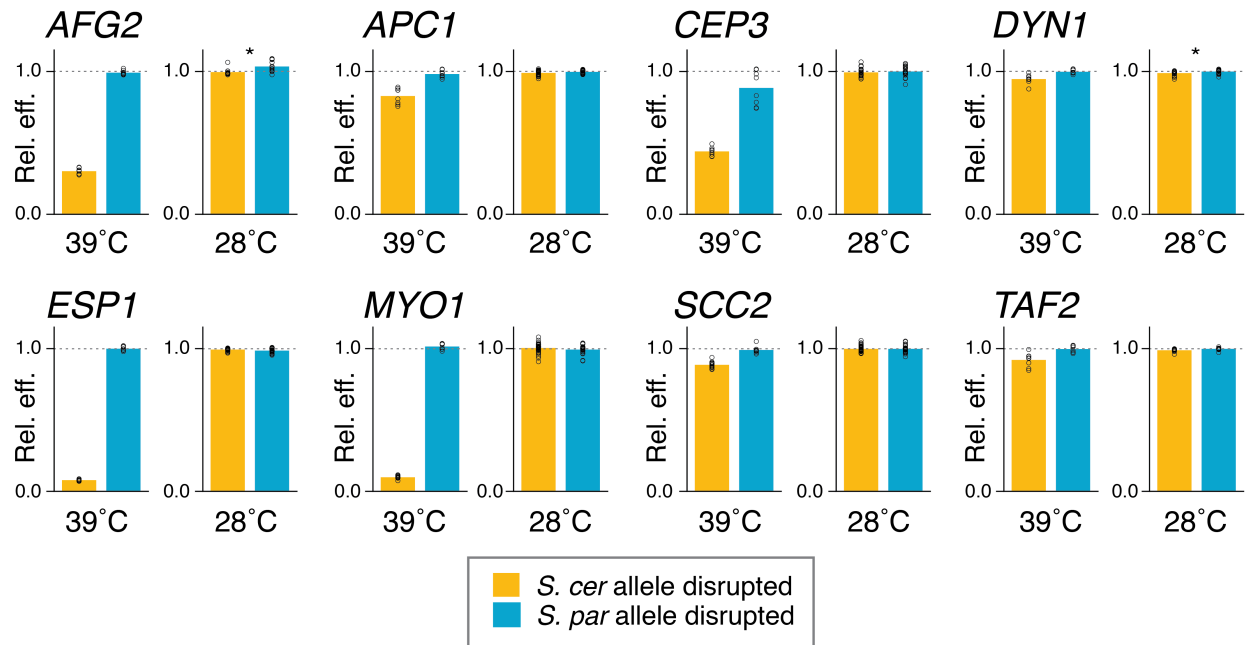


B



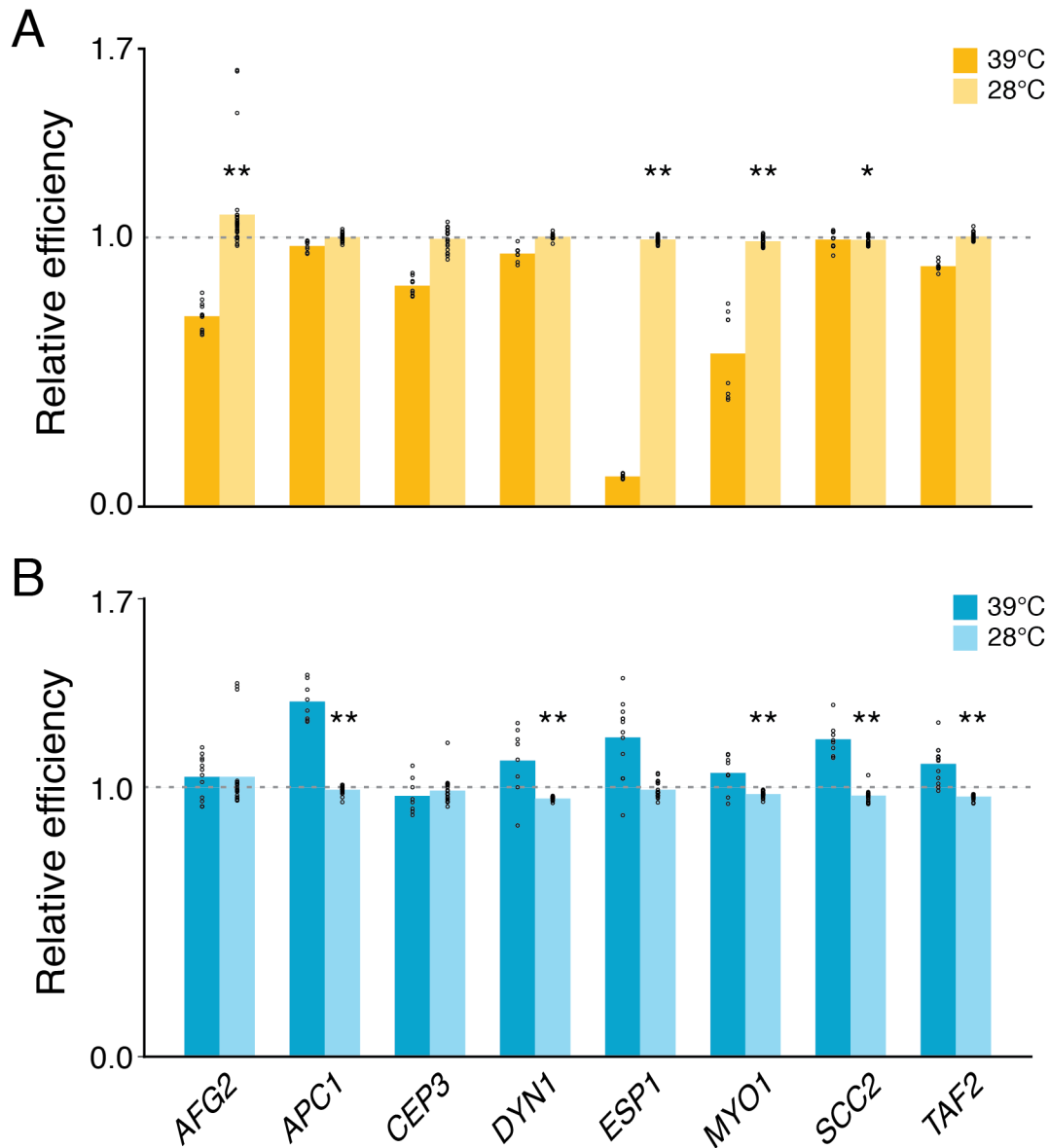
Supplementary Figure 6. RH-seq transposon coverage across the genome. A, Each panel reports sites in which the PiggyBac transposon inserted in the indicated *S. cerevisiae* DBVPG1373 chromosome in clones of the *S. cerevisiae* DBVPG1373 x *S. paradoxus* Z1 hybrid, as mapped from a pool of such clones by RH-seq. Each point reports one insertion; the x-axis reports the chromosomal position of a given insertion site, and the y-axis reports the raw number of sequencing reads mapped to that site. Colored tick marks along the bottom of each panel report genomic features that prohibited the mapping of reads. Read counts are from a representative RH-seq library after seven generations of culture at 39°C, reflecting the abundance in the pool of the respective hemizygote clone harboring the insertion. **B,** Data are as in **A**, except that shown are results from transposon insertions along *S. paradoxus* Z1 chromosomes in the *S. cerevisiae* x *S. paradoxus* hybrid.

Supplementary Figure 7



Supplementary Figure 7. Variation at RH-seq hit loci has little impact on growth at 28°C in the background of the interspecific hybrid. Each panel reports growth efficiency measurements of targeted-deletion reciprocal hemizygotes at the indicated RH-seq hit locus. In a given panel, the left-hand pair of bars reports relative efficiencies of targeted-deletion hemizygotes after culture at 39°C, from Figure 2B of the main text. In the right-hand pair of bars, each bar reports the mean growth efficiency ($n \geq 12$) after culture at 28°C of a targeted-deletion hemizygote in the indicated species' allele, normalized by the analogous quantity for the wild-type hybrid parent; individual measurements are reported as open circles. Statistical analyses of 39°C efficiency data are reported in Figure 2; *, $p \leq 0.05$, in a test for a difference in efficiency between the indicated hemizygotes at 28°C.

Supplementary Figure 8

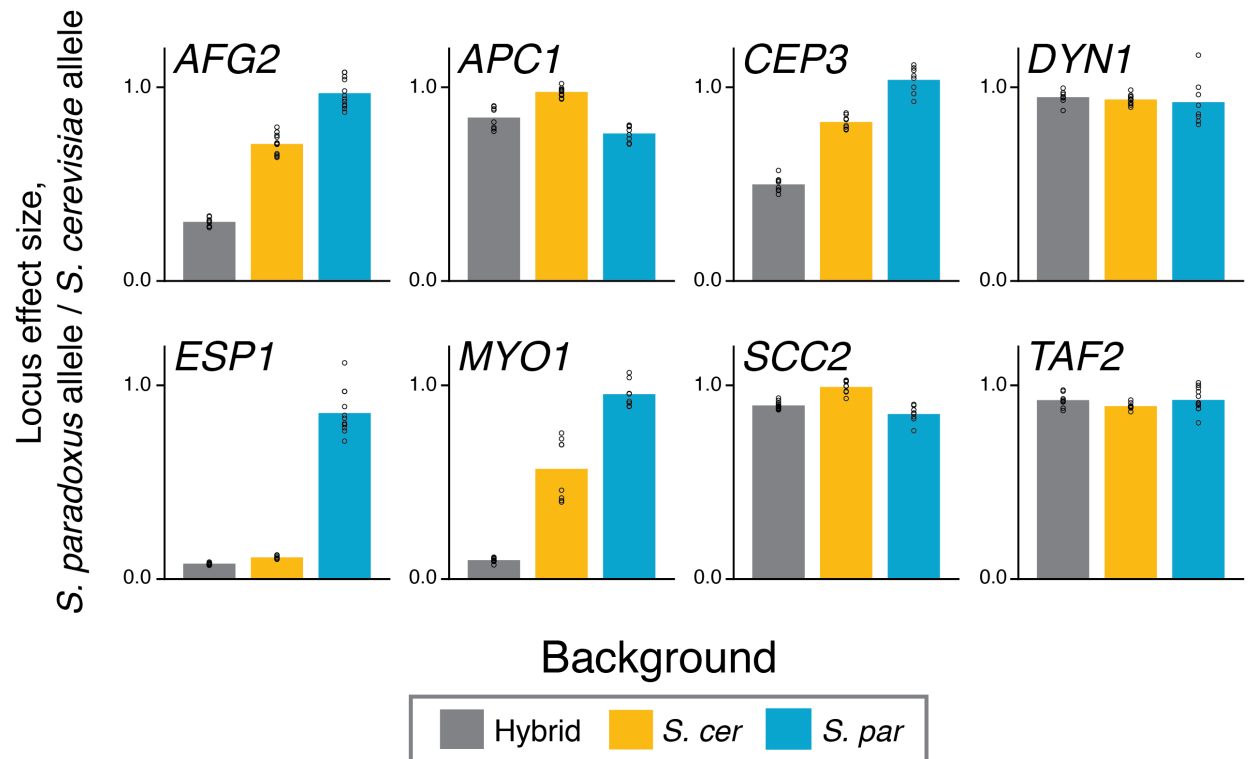


Supplementary Figure 8. Variation at RH-seq hit loci has little impact on growth at 28°C in

the background of the purebred species. A, Each pair of bars reports measurements of growth efficiency of an *S. cerevisiae* DBVPG1373 strain harboring the *S. paradoxus* Z1 allele at the indicated RH-seq hit locus, relative to the analogous quantity for wild-type *S. cerevisiae* DBVPG1373. The dark-shaded bar reports mean relative efficiency of the allele-replacement strain after culture at 39°C, from Figure 3 of the main text. The light-shaded bar reports mean

growth efficiency ($n \geq 11$) of the allele replacement strain after culture at 28°C, relative to the analogous quantity for wild-type *S. cerevisiae* DBVPG1373; individual measurements are reported as open circles. Statistical analyses of 39°C efficiency data are reported in Figure 3; *, $p \leq 0.05$ and **, $p \leq 0.01$, in a test for a difference in efficiency at 28°C between the indicated allele-replacement strain and the wild-type *S. cerevisiae* DBVPG1373. **B**, Data and symbols are as in **A**, except that each bar reports results from a *S. paradoxus* Z1 strain harboring the *S. cerevisiae* DBVPG1373 allele at the indicated locus, relative to wild-type *S. paradoxus* Z1.

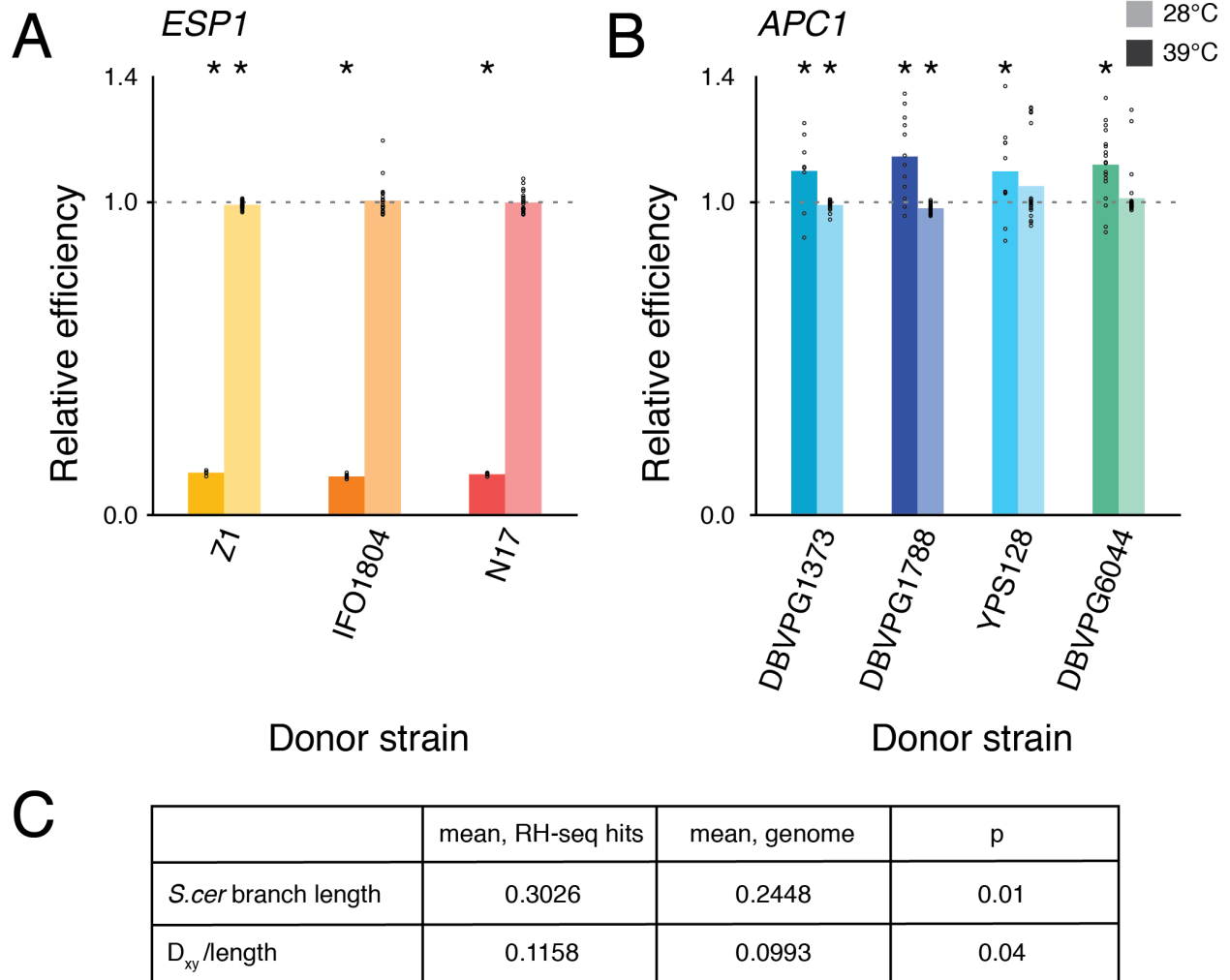
Supplementary Figure 9



Supplementary Figure 9. Effect sizes of thermotolerance loci depend on genetic background. Each panel reports a comparison of the impact on thermotolerance of allelic variation at the indicated gene, in the indicated diploid backgrounds. In a given panel, the grey bar reports the growth efficiency at 39°C of a hybrid strain harboring a wild-type copy of the allele from *S. paradoxus* Z1 of the focal gene and a full deletion of the allele from *S. cerevisiae* DBVPG1373, normalized by the analogous quantity measured in a hybrid with a wild-type *S. cerevisiae* allele and a deletion in the *S. paradoxus* allele, from the insets of Figure 2 of the main text. The orange bar reports the growth efficiency at 39°C of a strain of the *S. cerevisiae* DBVPG1373 background harboring the allele from *S. paradoxus* Z1 of the focal gene, normalized by the analogous quantity measured in wild-type *S. cerevisiae* DBVPG1373, from Figure 3A of the main text. The blue bar reports the growth efficiency at 39°C of wild-type *S. paradoxus* Z1, normalized by the analogous quantity measured in a strain of *S. paradoxus* Z1

harboring the allele from *S. cerevisiae* DBVPG1373 of the focal gene, from Figure 3B of the main text. Individual measurements are reported as open circles.

Supplementary Figure 10



Supplementary Figure 10. At RH-seq hit loci, the effect of allelic variation is conserved

across a given species, and sequence divergence from *S. paradoxus* is a common

feature of *S. cerevisiae* strains. A, Each pair of bars reports growth efficiency of an *S.*

cerevisiae DBVPG1373 strain harboring the allele of *ESP1* from the indicated strain of *S.*

paradoxus, relative to the analogous quantity for wild-type *S. cerevisiae* DBVPG1373; heights of

the dark and light bars report mean relative efficiency at 39°C ($n = 4-22$) and 28°C ($n = 11$),

respectively. Individual measurements are reported as open circles. **B,** Data and symbols are as

in **A**, except that each bar reports results from a *S. paradoxus* Z1 strain harboring the allele of *APC1* from the indicated strain of *S. cerevisiae*, relative to wild-type *S. paradoxus* Z1. *, $p \leq 0.034$ in a test for a difference in efficiency between the indicated allele-replacement strain and 1. Provenance of each strain is as follows: Z1, oak bark, UK; N17, oak exudate, Russia; IFO1804, oak bark, Japan; DBVPG1373, soil, Netherlands; DBVPG1788, soil, Finland; YPS128, soil, USA; DBVPG6044, bili wine, West Africa. **C**, Each row reports a comparison of the sequences of RH-seq hit loci against a genomic null. *S. cer* branch length, number of sequence substitutions along the lineage leading to *S. cerevisiae*, in a phylogenetic tree inferred from *Saccharomyces* species type strains. D_{xy}/length , average number of differences between the *S. paradoxus* type strain and a strain randomly chosen from the *S. cerevisiae* wine/European population, normalized by gene length. The first and second columns report the average of the indicated statistic across the eight RH-seq hit loci and across sets of eight loci randomly resampled from the genome, respectively. The third column reports the empirical p -value from a test for an elevated value of the indicated statistic relative to the resampling null.

Supplementary table captions

Supplementary Table 1. Strains used in this study. **A**, Wild-type diploid strains used, including those used as parents of the *S. cerevisiae* x *S. paradoxus* hybrid and of allele-replacement transgenesis; SGRP, the Saccharomyces Genome Resequencing Project, version 2. **B**, Hemizygotes in the *S. cerevisiae* DBVPG1373 x *S. paradoxus* Z1 diploid hybrid constructed by targeted deletion of a given species' allele of the indicated gene with the KanMX or NatMX cassette. Δ scYFG::KanMX/spYFG signifies that the *S. cerevisiae* DBVPG1373 allele of YFG was knocked out and the *S. paradoxus* Z1 allele of YFG is intact; strains with the DBVPG1373 allele intact and the Z1 allele knocked out are represented analogously. **C**, Allele replacement strains in *S. cerevisiae* DBVPG1373 or *S. paradoxus* Z1 diploid homozygote backgrounds. In genotype notes, e.g. in an *S. paradoxus* background, Δ YFG(-X to +Y)::scYFG(-Z to +W) indicates that in *S. paradoxus* Z1, bases -X to +Y from gene YFG have been removed and replaced by bases -Z to +W of the allele of YFG from the indicated *S. cerevisiae* strain. Positive coordinates count in the 5' to 3' direction from the start codon (+1 corresponds to the A in the ATG), and negative coordinates count in the 3' to 5' direction from the start codon (-1 corresponds to the base directly 5' of the ATG). In cases where the replacement extended into a region of 100% conservation between species, the position of the last divergent nucleotide is shown.

Supplementary Table 2. Depth of RH-seq library sequencing. Each row reports the number of sequencing reads, before mapping, from an RH-seq library made from the DNA of transposon mutant hemizygotes in the *S. cerevisiae* DBVPG1373 x *S. paradoxus* Z1 diploid hybrid. The last four rows report results from the pool immediately after transposon

mutagenesis, mutant clone isolation, pooling, and pre-growth at 28°C (time zero, T0). The first 24 rows report results from selection (bulk culture of the pool) at the indicated temperature after inoculation from the T0 sample.

Supplementary Table 3. Abundances of transposon-mutant clones in the interspecific hybrid from RH-seq. Each row reports results of sequencing one transposon insertion in the *S. cerevisiae* DBVPG1373 x *S. paradoxus* Z1 diploid hybrid after selection of the transposon mutant pool, reflecting the abundance in the pool of the respective hemizygote clone harboring the insertion. Allele, the species parent's homolog in which the transposon insertion lay. Chromosome, strand, location, and gene, the fine-scale position of the insertion. Abundance, read counts of the transposon insertion sequenced after selection of the mutant pool at the indicated temperature, normalized for library size and averaged across biological and technical replicates. Transposon insertions not detected in any replicate of the indicated selection were assigned an abundance of 1. CV, coefficient of variation over biological replicates of normalized read counts after selection at the indicated temperature.

Supplementary Table 4. Tests of the impact on thermotolerance of variation at each gene in turn via reciprocal hemizygote analysis of clone abundances from RH-seq. Each row reports the results of reciprocal hemizygote tests of thermotolerance of hemizygote transposon mutants at the indicated gene in the *S. cerevisiae* DBVPG1373 x *S. paradoxus* Z1 diploid hybrid. The second, third, and fourth columns report results of a Mann-Whitney statistical test for a difference in the abundance after growth at 39°C, relative to the abundance after growth at 28°C, of hemizygotes harboring transposon insertions in the two species parents' homologs. The last two columns report the log ratio of normalized abundances of a hemizygote harboring a

transposon insertion in the indicated species parent's homolog after culture at 39°C and 28°C, as a geometric mean across transposon mutants from Supplementary Table 3.